A piston ring pack tribological design for internal combustion engines

Anastasios Zavos[†], Pantelis G. Nikolakopoulos[*,1]

[†] Machine Design Laboratory, Department of Mechanical Engineering and Aeronautics,
University of Patras, Greece
zavosa@mech.upatras.gr

[*]Machine Design Laboratory, Department of Mechanical Engineering and Aeronautics,
University of Patras, Greece
pnikolak@mech.upatras.gr

ABSTRACT

The design of piston ring pack is a major subject on the internal combustion engines. The current trend focused on thin piston rings and the improvements of profile to oil consumption and lubrication in each engine stage. In this paper, an investigation of piston ring shapes in modern combustion engines was performed. The geometrical dimensions of piston ring pack-cylinder tribo pair were obtained from a four stroke motor engine. A 2D axisymmetric model of ring pack-cylinder was created using the finite element method. The minimum oil thickness, the combustion gas pressures and the asperities contribution were updated for each crankshaft position in quasi static manner. The fluid field was solved based on the Navier Stokes approach, as well as the piston ring balance was performed. Several shape profiles for top ring were examined and compared. Lower curvature height improved the minimum lubricant thickness, thus the total friction force decreased near to top dead center.

Keywords: *piston rings, total friction force, hydrodynamic pressure, oil thickness, profile, top dead center*

L : stroke length (m)
D_{ring} : piston ring diameter (m)
D_{cyl} : cylinder diameter (m)
V : piston linear velocity (m/s)
d : piston groove end length (m)
p_{hyd} : local hydrodynamic pressure (Pa)
p_c : combustion pressure (Pa)
p_1 : gas pressure on the top land of piston (Pa)
p_2 : inter ring pressure for second land (Pa)
p_3 : inter ring pressure for third land (Pa)
Ω : rotational crankshaft speed (rpm)
T_{TDC} : cylinder liner temperature at the top dead center (TDC) (^oC)
T_{BDC} : cylinder liner temperature at the bottom dead center (BDC) (^oC)
T_{mid} : cylinder liner temperature at the mid-stroke position (^oC)
T_{oil} : oil temperature (^oC)
φ : crank angle (degree)
μ : dynamic viscosity (Pas)
F_{total} : total friction force (N)
F_b : boundary friction force (N)
F_{fl} : fluid friction force (N)
h_{min} : minimum oil thickness (μm)
$h(y,t)$: oil film thickness (μm)

[1] Corresponding author: Pantelis G. Nikolakopoulos, +30 2610 969421, e-mail : pnikolak@mech.upatras.gr

1 Introduction

The interaction of piston rings and cylinder inner liner has been numerical and experimental investigated by many researchers, in order to understand the main design issues, such as the friction losses, the oil consumption and the surface contact behavior. The analysis of piston assembly pack under boundary/mixed and hydrodynamic conditions is a key for re-design of engine components. Therefore, the contribution of the current paper is focused on piston ring shape and its behavior with the cylinder wall.

One of the relative works which has to do with the piston ring profile and cylinder liner contact was made by Yeng [1]. Based on the Reynolds equation, the effects of piston ring curvature examined for two types of piston rings and the minimum oil thickness compared for each ring shape. Simultaneously, Dellis [2] examined the friction force with the use of a single ring test-rig taking into account the oil properties, the film thickness and the piston ring curvature. Results, for used and new piston rings presented and discussed. Additionally, a numerical approach for a worn and new profile ring is developed by Chong et. al [3]. Regarding the geometry of ring profile the cavitation zone investigated and the minimum oil film illustrated.

At the same time, simulation models of compression piston ring-cylinder system were presented by Zavos and Nikolakopoulos [4-6]. In our recent papers [4, 5], the mechanism of friction on a top smooth and wavy piston ring has been carried out in elasto-hydrodynamic conditions, utilized the Navier Stokes equations. The lubricant film velocity, the maximum oil thickness and the mechanical stresses on the piston ring were examined for several gas pressure leaks sub models [5]. Thereafter, the effect of lubricant oil on the friction in a real motor engine was investigated. The Strain gauge method was used for friction force measurement [6]. Afterwards, comparisons of experimental predicted and numerically calculated friction force was done and it was observed a good agreement.

Agostino et. al [7] developed also a simulation model for the top ring-cylinder contact. In their work, the authors have sought to identify the piston ring friction losses due to the oil viscosity, the engine operating conditions and the ring surface treatments. Morris et. al [8] presented a numerical model for transient and thermal mixed lubrication conditions of first piston ring. Their study developed a novel control volume thermal mixing model, showing that the rise in the lubricant oil temperature through shear is much less than the liner temperature. Recently, a novel approach based on Navier Stokes equations including the Rayleigh-Plesset model investigated by the authors Shahmohamadi et. al [9, 10]. The effect of asperities in thin oil films proposed regarding the Greenwood-Tripp model. Finally, a cavitation zone along to piston ring liner is provided.

The present paper presents a 2D axisymmetric piston ring pack model for a real four stroke motor engine located at the Machine Design Laboratory of the University of Patras. The model describes the gas pressures leakage for each ring taking into account the mathematical model by Chong et. al [3]. The fluid domain taking into account the ring balance into the piston groove is solved in a quasi static equilibrium analysis. The oil viscosity is considered as a function of cylinder's liner temperature. Different profiles of top ring were examined and discussed. The evaluation of total friction force and minimum lubricant film for each shape is also studied around top dead center (TDC).

2 Simulation Model

The lubrication performance of piston ring pack is affected by the oil supply, which is related to the gas pressures, the asperities contact and the lubricant thickness. In this case, the basic dimensions of piston assembly system were measured from a four stroke motor engine 107 cc located at Machine Design Laboratory. The main specifications of four stroke motor engine illustrated in Table 1.

Table 1. Motor engine specifications

Type	4-stroke, air cooled
bore* stroke	0.0524* 0.0495 m
rotational speed	1000 rpm
compression ratio	10:1
displacement	107 cc
piston groove end length	0.0002 m

2.1 Gas Pressure Model of Piston-Piston ring pack

This motor engine consists of two compression rings and one oil control ring. In practical terms, the first compression ring is operated under extreme conditions, and this is one more reason to improve its design and its lubrication performance. Figure 1 shows the type of piston rings of the motor engine and the variation of gas pressures. The main dimensions of piston-ring pack were measured by a 3D coordinate measuring machine.

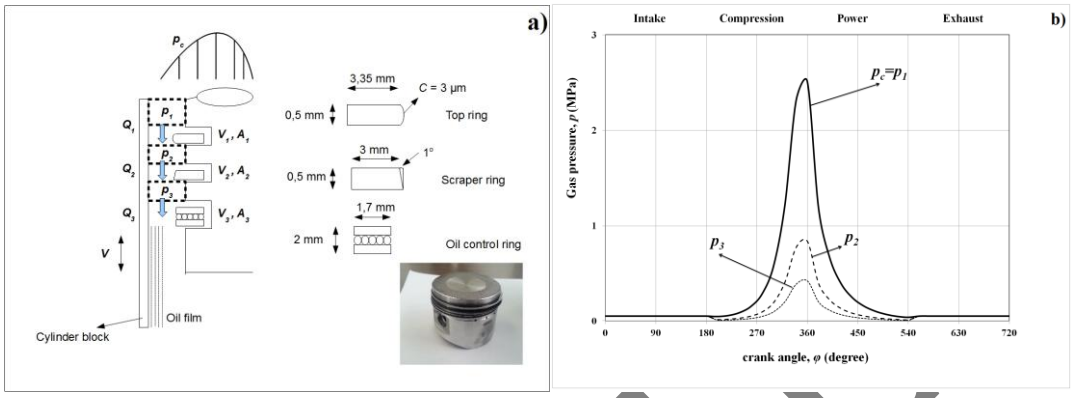

Figure 1: (a) Piston assembly geometry of four stroke motor engine, (b) the variation of gas pressures

For this analysis, the combustion gas pressure of a four stroke motor engine is calculated by ref. [12]. Continuing, a sub model of gas pressure leakage between control volumes through the ring end-gaps is developed and ilustrated in Figure 1. This method of gas flow have been developed analytically by Chong et. al [3]. Therefore, the prediction of each ring pressure is obtained according to the mathematical model of ref. [3]. It takes also into acount the mass flow rates { Q_1, Q_2, Q_3 } between each ring clearance,and the gas flow is considered ideal.

2.2 Temperature and Lubricant viscosity

The temperature along the cylinder liner plays an essential role in lubricant's oil performance. In this study, the motor engine is operated at a low rotational speed Ω = 1000 rpm cooled by an air-condition at 18 ^{o}C. SAE 30 was used as lubricant and the temperature variation is illustrated using a high performance thermo camera type: FLIR SC660 with 640×480 resolution and ±1% accuracy. Figure 3 (a) shows a picture of liner temperature for Ω = 1000 rpm under warmed conditions. According to Morris work [8], the increment of oil temperature through shear is slighter than the liner temperature; hence the oil temperature is the same with the cylinder's liner temperature at each position. Therefore, the oil temperature can be estimated using the measured temperatures in this analysis. As it is observed the temperature variation can be considered as, T_{TDC} = 43 ^{o}C , T_{BDC} = 38 ^{o}C and T_{mid} =40 ^{o}C. The dynamic viscosity can be described as a function of oil temperature according to the Vogel's equation (1) and it is presented in Figure 3 (b).

$$\mu(T_{oil}) = \alpha_o \exp\left(\frac{\theta_1}{\theta_2 + T_{oil}}\right) \quad (1)$$

where a_o = 0.048 mPas, θ_1 =1123.35 ^{o}C, θ_2 = 111.65 ^{o}C are the relevant parameters for monograde SAE 30 and T_{oil} is the oil temperature.

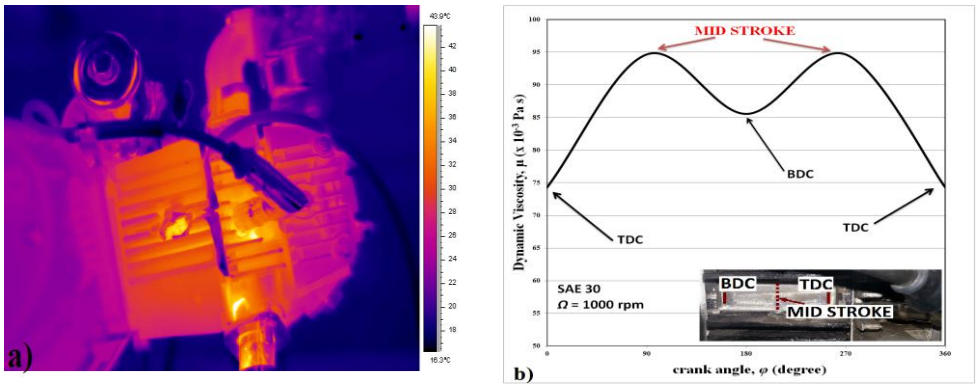

Figure 3: (a) A snapshot of cylinder liner temperature for low speed Ω = 1000 rpm, (b) oil film viscosity vs crank angle.

2.3 Modeling of Oil thickness

The sensitivity of lubricant thickness is strong correlated with the piston ring shape and the operation engine conditions. In this study, the minimum oil film h_{min} is defined based on the piston ring balance criterion. In Figure 4 a sketch of the piston ring profile contact along to cylinder inner liner is illustrated.

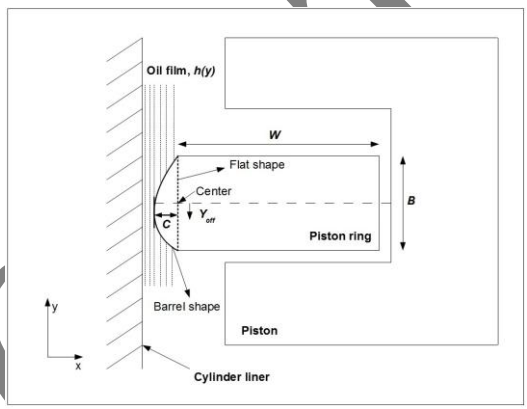

Figure 4: Piston ring shape contact and the oil film thickness

The lubricant film thickness between the ring profile and the cylinder inner liner is given by:

$$h(y,t) = h_{\min}(t) + \underbrace{\frac{C}{\left(\frac{B}{2} + Y_{off}\right)^2}(y - Y_{off})^2}_{h_s(y)} + \delta_r + \delta_{cyl} \qquad (2)$$

where $h_{min}(t)$ is the minimum oil thickness of piston ring-cylinder contact at any time, $h_s(y)$ is the piston ring face shape and δ_r , δ_{cyl} is the surface roughness amplitude for the ring and the cylinder accordingly. The local asperity elastic deformation is not considered in equation (2). Actually, the hard coating (Cr) around the ring thickness showed insignificant elastic deformation.

3 Assumptions and Governing Equations

A 2D axisymmetric piston ring pack model is created. The contact between the piston ring and cylinder liner is observed around the dead centers, under the consideration of mixed/hydrodynamic conditions. Afterwards, it is important to refer the following assumptions:

1. The flow is considered laminar and two dimensional.
2. Ring twist and flutter into the piston groove are ignored.

3. Body forces are considered and the piston – cylinder model is assumed to be concentric assembled.
4. The oil viscosity is a function of liner temperature.
5. The top piston ring moved in the axial direction according to the piston speed *V* in the y-axis.

A 2D axisymmetric model is developed using the computational fluid dynamics (CFD). The Navier Stokes equations, momentum equation (3), coupled with the continuity equation (4), are solved using the finite volume method.

$$\frac{\partial}{\partial t}(\rho\vec{v})+\nabla\cdot(\rho\vec{v}\vec{v})=-\nabla p+\nabla\cdot\left(\bar{\bar{\tau}}\right)+\rho\vec{g}+\vec{F} \quad (3), \qquad \frac{\partial\rho}{\partial t}+\nabla\cdot(\rho\vec{v})=0 \quad (4)$$

where $\rho\vec{g}$ and $\vec{F}$ are the gravitational body force and external body forces. The stress tensor can be expressed as:

$$\bar{\bar{\tau}}=\mu\left[\left(\nabla\vec{v}+(\nabla\vec{v})^{T}\right)-\frac{2}{3}\nabla\cdot\vec{v}\bar{\bar{I}}\right] \quad (5)$$

where the second term on the right hand side is the effect of volume dilation and μ is the dynamic viscosity.

3.1 Asperity contact model

Asperities contact may substantially affect the piston ring performance when the oil film thickness is comparable with the roughness height. Thus, a part of the ring profile influenced by the asperities contact. In the present study, the Greenwood and Tripp model was studied for the asperities interaction between the ring and the cylinder. The asperity height distribution is Gaussian, since the average contact pressure p_{cont} and the real area of contact A_{cont} are given by the following equations:

$$p_{cont}=\frac{8\sqrt{2}}{15}\pi(\zeta\kappa\sigma)^{2}\sqrt{\frac{\sigma}{\kappa}}E'F_{5/2}(\lambda) \quad (6) \text{ and } A_{cont}=\pi^{2}(\zeta\kappa\sigma)^{2}AF_{2}(\lambda) \quad (7)$$

The statistical functions $F_{5/2}(\lambda)$, $F_2(\lambda)$ are obtained as a relation of the Stribeck oil film parameter ($\lambda = \frac{h(y,t)}{\sigma_{rms}}$) . The Gaussian statistical functions defined as: $F_j(\lambda)=\frac{1}{2\pi}\int_{\lambda}^{\infty}(s-\lambda)^{j}e^{-\frac{s^2}{2}}ds$ (8)

For this analysis, the authors Hu et al. [11] used a non-linear curve; thus the function $F_{5/2}(\lambda)$ is solved more easily. In more detail, this expression separated at two parts as follows:

$$F_{5/2}(\lambda)=\begin{cases}\mathrm{A}(\Omega-\lambda)^{z}\rightarrow\lambda\le\Omega\\ 0\rightarrow\lambda>\Omega\end{cases} \quad (9)$$

where the above parameters considered Ω = 4, A = 4.4068 10^{-5} and z = 6.804. In more detail, Hu et. al [11] utilized the oil film parameter with the upper level λ = 4 in the mixed conditions. Finally, the main geometrical dimensions of piston rings-cylinder system obtained from a TESA 3D CMM. Table 2 lists the basic topographical parameters for two compression rings and the cylinder wall.

Table 2. Topographical parameters of four stroke motor engine

Parameters	Value
Top ring roughness	0.35 μm
Scraper ring roughness	0.25 μm
Cylinder liner roughness	0.1 μm
roughness parameter $\zeta\kappa\sigma_{rms}$	0.123
Asperity slope σ_{rms}/κ	1.565 10^{-3}

4 Boundary conditions

This model simulates the hydrodynamic force, the elastic ring tension and the asperity contact on piston ring pack-cylinder system. The radial motion of the piston rings was represented by the lubricant oil thickness. Therefore, the algorithm was updated in a quasi-static manner for each crankshaft position taking into account the piston linear speed, the minimum oil film, the gas pressures and the asperity load. The inlet and outlet pressures are p_c and $p_{out} = p_{atm}$, depending on the direction of piston movement. In equation (10) the back pressure p_{bk} at the ring gap is equivalent to the combustion pressure. Figure 5 illustrates the applied forces on the top piston ring. Steel piston rings and aluminium cylinder considered in this analysis.

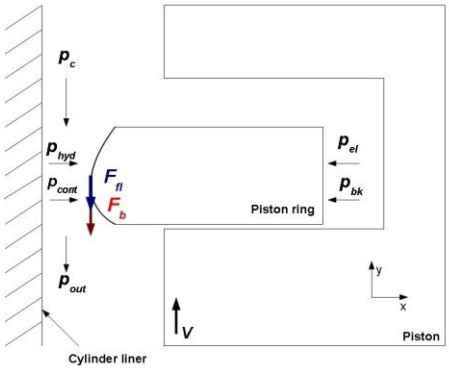

Figure 5: Piston ring geometry with applied forces.

The elastic pressure $p_{el} = \frac{dEI}{3\pi Br_{cyl}^4}$ and the pressure contact by the asperities p_{cont} are calculated separately. Thereafter, the convergence criterion of the pressure balance was used according to the equation (10). If this criterion is not confirmed, then the minimum oil thickness h_{min} is redefined and the interaction loop of lubricant thickness (11) is repeated. The value of ε=0.03 is given in the numerical parameter ε (equation 11) in order to perform simulations here.

$$X = \left| \frac{\left[p_{cont}(\varphi) + p_{hyd}(\varphi) \right] - \left[p_{el} + p_{bk}(\varphi) \right]}{\left[p_{el} + p_{bk}(\varphi) \right]} \right| \leq 0.2\% \quad (10), \text{ and } \frac{h_{\min}^{N+1} - h_{\min}^{N}}{h_{\min}^{N}} = \varepsilon X_{\max}, \text{where } N \geq 1 \quad (11)$$

4.1 Fluid Algorithm Implementation and Meshing

Figure 6 illustrates the steps of simulation solution and the computational grids of fluid domain. Regarding the fluid field, tetrahedral elements are used. According to the relevant published works [5, 6], ten divisions were used in the radial direction and 500 divisions were used in the axial direction. It should be noted that this configuration of fluid meshing shown a very good conformance with the results of Shahmohamadi et. al [10]. Continuing, the convergence criteria were activated relative to the pressure error [4-6] and the ring balance convergence criterion is also used as it is discussed in paragraph 4.

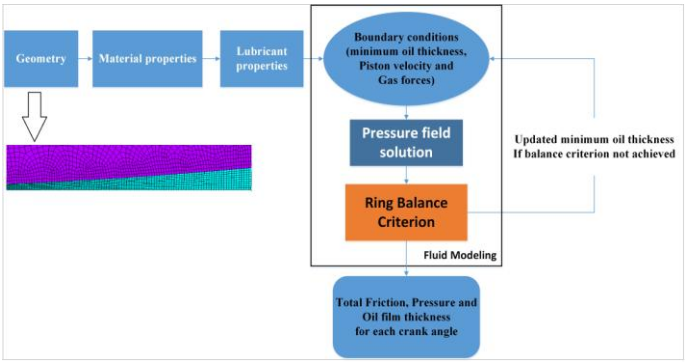

Figure 6: Fluid algorithm solution and the fluid discretization

4.2 Total Friction Force

The total friction force is obtained as a sum of the viscous friction because of the oil film interface and the boundary friction due to asperity interactions along to piston ring profile. The contribution of mixed/hydrodynamic regime on the piston ring-cylinder contact has been shown by the analytical expression (12). It is important to refer that the non-Newtonian Eyring shear stress τ_o and the boundary shear strength of the surfaces, named ς, have been taken from refs. [8, 10].

$$F_{total} = F_{fl} + F_b \Rightarrow F_{total} = \int_{A-A_{cont}} \bar{\tau} d(A - A_{cont}) + \tau_o A_{cont} + \varsigma \int p_{cont} dA \quad (12)$$

5 Results and Discussion

5.1 Fluid Modeling Validation

The pressure distribution along to piston ring thickness compared with the numerical data of Shahmohamadi et. al [10]. As follows from Figure 7, the predicted pressure field by the current has a very good agreement ($Press_{error} \leq 5\%$) with those of ref [10]. In more detail, these validated results were obtained for a barrel piston ring at crank angle (φ = -5°) when the piston moves upwards and the balance confirmed for minimum oil thickness h_{min} = 0.39 μm as obtained from the equation (11).

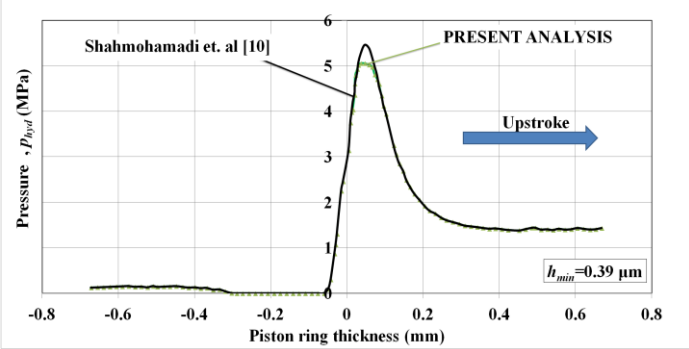

Figure 7: Validation results from Shahmohamadi et. al [10].

5.2 Effect of the Piston ring Curvature

Figure 8 illustrates the pressure profile of first compression ring at different curvatures. The top ring behaviour is simulated at reversal point (TDC), where the boundary/mixed lubrication occur. As observed the pressure and the oil distribution change by varying the ring profile curvature. For example, the maximum pressure is increased substantially 26.7% when the curvature becomes higher from C = 3 μm, Y_{off} = 0 to C = 20 μm, Y_{off} = 0. Also, it is clear that the "*flatter*" profile increases the minimum oil film thickness; hence the total friction force is reduced. As indicated in Table 3, the top ring with the curvature of C = 3 μm, has a minimum value regarding the boundary friction. The minimum lubricant thickness is increased in a value of h_{min} = 0.68 μm, in comparison with the ring's curvature of C = 20 μm. Hence, a higher curvature height leads to a thinner oil film near the TDC; since the boundary lubrication is enhanced.

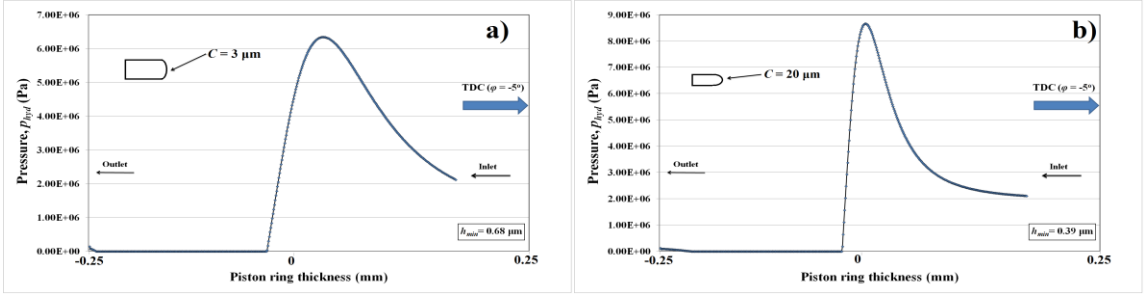

Figure 8: Hydrodynamic pressure for different curvatures of top ring near the TDC.

Table 3. Total friction force of top ring near the top dead center (TDC).

Parameters: (C, Y_{off})	**F_{fl} (N)**	**F_b (N)**
C = 3μm, Y_{off} = 0	16.39	1.70
C = 20 μm, Y_{off} = 0	18.33	15.36

6 Conclusions

In the current paper a 2D axisymmetric model of piston-ring pack from a real four stroke motor engine is developed. Lower curvature height leads to a higher film thickness at the top dead center (TDC). In fact, the carrying load capacity of the ring profile changes the oil film distribution near to the reversal points. To this point, "*flatter*" ring shape tends to an "optimum" minimum lubricant thickness giving zero friction force in boundary lubrication regime.

Acknowledgement

This work was supported by Grant E.039 from the Research Committee of the University of Patras (Programme K. Karatheodori).

References

1. Jeng Y. (1992). Theoretical Analysis of Piston-Ring Lubrication Part 1-Fully Flooded Lubrication. *STLE Tribol. Trans.*, 35, 696–706.
2. Dellis P.S. (2010). Effect of friction force between piston rings and liner: a parametric study of speed, load, temperature, piston-ring curvature, and high-temperature, high-shear viscosity. *Proceedings of the Institution of Mechanical Engineers, Part J: Journal of Engineering Tribology*, 224, 411-426. doi: 10.1243/13506501JET727
3. Chong W.W.F., Howell-Smith S., Teodorescu M., Vaughan N.D. (2013). The influence of inter-ring pressures on piston-ring / liner tribological conjunction, *Proceedings of the Institution of Mechanical Engineers, Part J: Journal of Engineering Tribology*, 227, 154-167.
4. Zavos A., Nikolakopoulos P. (2015). Effects of Surface Irregularities on Piston Ring-Cylinder Tribo Pair of a Two Stroke Motor Engine in Hydrodynamic Lubrication. *Tribology in Industry*, 37(1), 1-12.
5. Zavos A., Nikolakopoulos P.G. (2015). Waviness and straightness of cylinder and textured piston ring tribo pair. *International Journal of Structural Integrity*, 6(2), 300 - 324.
6. Zavos A., Nikolakopoulos P.G. (2015). Effects of Monograde and Multigrade Oils on the Friction Force in Four-Stroke Motor Engine: An Experimental and Analytical Approach. In book: *Vibration Engineering and Technology of Machinery*, Springer International Publishing, 23, 507-517. doi: 10.1007/978-3-319-09918-7_45
7. Agostino V.D', Maresca P., Senatore A. Theoretical analysis for friction losses minimization in piston rings, *Proceedings of the International Conference on Tribology*, Parma, Italy, 20-22.09.2006.
8. Morris, N., Rahmani, R., Rahnejat, H., King, PD., Fitzsimons, B. (2013). Tribology of piston compression ring conjunction under transient thermal mixed regime of lubrication, *Tribology International*, 59, 248-258.
9. Shahmohamadi, H., Rahmani, R., Rahnejat, H., Garner, C.P., King, P.D. (2013) Thermo-mixed hydrodynamics of piston compression ring conjunction. *Tribology Letters*, 51, 323-340.
10. Shahmohamadi, H., Rahmani, R., Rahnejat, H., Garner, C. P. (2013). CFD modelling of cavitation phenomenon in piston ring/cylinder liner conjunction. *In 5th World Tribology Congress (WTC 2013)*, Torino, Italy, September 8-13 (p. 4).
11. Hu, Y., Cheng, H. S., Arai, T., Kobayashi, Y., & Aoyama, S. (1994). Numerical simulation of piston ring in mixed lubrication—a nonaxisymmetrical analysis. *Journal of Tribology*, 116(3), 470-478.
12. Richard Stone. Introduction to Internal Combustion Engines, 3rd Edition, Macmilan Press Ltd, 1999.